OPTIMISATION OF JET STEADY-STATE ELMY DISCHARGES WITH ITER-RELEVANT DIVERTOR CONDITIONS

The JET Team[1]
(Presented by D Stork)

JET Joint Undertaking,
Abingdon, Oxfordshire,
United Kingdom.

Abstract

Experiments with the JET Mark IIA divertor involving optimisation of performance with gas fuelling are discussed. The development of plasmas in the Mark IIA configuration at high current ($\geq$ 4.5MA) and low q ($q_{95} \leq 2.6$) is presented. The results of a preliminary experiment to study the dimensionless (ρ^* and ν^*) scaling of energy confinement in impurity-seeded plasmas with high radiated power are discussed. It is found that the energy confinement is not consistent with gyro-Bohm scaling and does not follow the ITERH93-P scaling law for ELM-free plasmas.

1. INTRODUCTION

JET is now in the middle of a programme designed to investigate the effect of divertor geometry on plasma performance. The configurations studied so far are the Mark I (Fig.1(a)) and the Mark IIA (Fig.1(b)). This series will conclude with an ITER-specific "Gas Box" (Mark IIGB) in 1997/98. The programme follows a progressively more closed series of configurations. Each of the divertors uses a cryopump with a nominal pumping speed (deuterium) of $240 m^3 \cdot s^{-1}$.

Optimisation of plasma performance in steady-state ELMy H-mode discharges in the Mark IIA divertor has concentrated on the effect of changes in plasma configuration and fuelling. Changes in bulk plasma parameters (such as plasma triangularity) and in divertor closure-related parameters (such as magnetic flux expansion at the target) are covered in a related paper [1] which also addresses the behaviour of type I ELMs in the Mark IIA. The changes in plasma performance due to main species (D_2) fuelling are discussed in Section 2 below.

The steady-state ELMy H-mode is a candidate for production of high performance (in terms of stored energy and fusion yield) plasmas in the forthcoming deuterium-tritium experiments in JET (DTE1) scheduled for early 1997. The optimisation of this regime at high current ($\geq$ 4.5MA) and full field ($3.4 \geq B_T \geq 3.1$T) in JET involves plasma operation at low values of q ($q_{95} < 2.6$) where experimental input would provide useful information for ITER operation. The status of this work is described in Section 3.

The highly-radiating impurity-seeded divertor plasmas which were first studied in JET in the Mark I campaign [2] have been the subject of further study in Mark IIA [1]. An important issue is whether the confinement quality of these discharges, which is barely acceptable for ITER [1,2] is maintained as the dimensionless variables (ρ^* and ν^*) are increased towards the ITER range. Investigations into this topic in Mark IIA are described in Section 4.

[1] See Appendix to IAEA-CN-64/O1-4, The JET Team (presented by J Jacquinot).

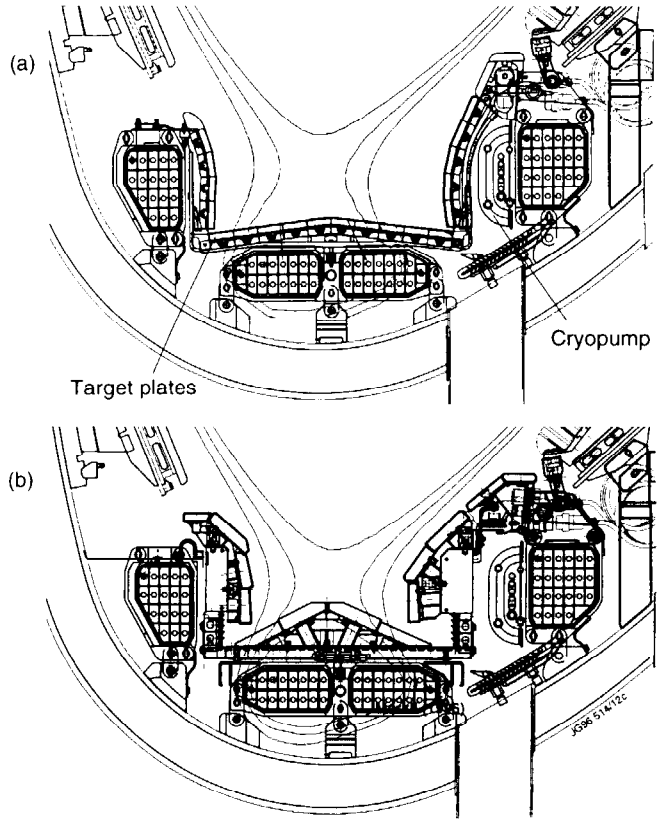

Fig.1 JET divertor geometries. (a) Mark I divertor (1994/95) (b) Mark IIA divertor(1996).

2. DIVERTOR PLASMA BEHAVIOUR WITH FUELLING VARIATIONS

2.1 Discharges with fuelling only from neutral beams

As with the Mark I divertor [3], steady-state discharges with Type I ELMs are routinely achieved in the Mark IIA divertor. The "natural" behaviour of discharges which are not fuelled by added gas, but only sustained by neutral beams and the input from edge recycling, has been extensively studied [1]. This natural behaviour can be summarised as follows:

- the type I ELMy H-modes have a similar confinement to Mark I plasmas with confinement enhancement (H_{93}) relative to the ITERH93-P ELM-free H-mode scaling of $0.9 \leq H_{93} \leq 1.1$ at plasma currents from 2.5-3.5MA;
- the discharges reach a steady-state density which for a fixed plasma configuration scales as

$$\langle n_e \rangle \propto \left(I_p \cdot P_{nbi}\right)^{0.5} / \pi a^2$$

  similar to the behaviour in Mark I but with a 15% lower density for similar configurations [4];
- the discharges have similar low fraction of radiated power (around 20% of input power) and moderate Z_{eff} (1.5-2.5). Z_{eff} is highest in discharges with higher triangularity, principally because of the reduced ELM frequency in such discharges [1]. Carbon is the predominant impurity.

2.2 Discharges with external deuterium gas fuelling

Heavy D_2 gas puffing (up to ~ 5 10^{22} atoms s^{-1}) has been applied to all the Mark IIA plasma configurations. The fuelling efficiency is lower than in Mark I. This is partly due to the fact that the rate of pumping in Mark IIA is higher than in Mark I [1], the Mark IIA geometry behaving as a moderate slot divertor by trapping the returning neutrals near the pumping ports.

The fuelling efficiency is found to be independent of the location of the gas feed. Fuelling in the upper vessel; in the private region; in the outboard midplane and at the inner and outer strike zones, all achieve the same asymptotic density for a given fuelling rate, plasma current and configuration.

As the fuelling is increased, the ELM frequency rises and the confinement begins to degrade [1]. The confinement degradation is correlated with an increase in the outer midplane pressure or outer midplane recycling, which rise due to the imperfect closure of the Mark IIA configuration. The same global behaviour was observed in Mark I [3,5]. The plasma density increases at first as fuelling is increased (Fig.2(a)) but eventually a maximum density is reached beyond which a further density rise is impeded because the ELMing rate continues to increase with increased fuelling and density is expelled. The maximum density is not accompanied by any dramatic fall in confinement (Fig.2(b)) which continues to decline slowly. The density limit appears to be related to poor fuelling efficiency as ionised neutrals are unable to convect into the plasma against the increasing ELM frequency. The limit is not associated with a disruptive or radiative collapse.

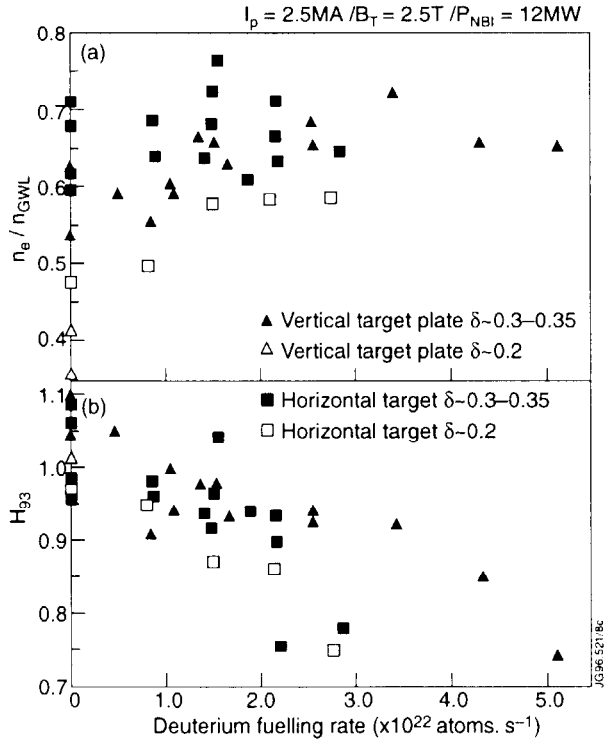

Fig.2 (a) Plasma density achieved (as a fraction of the Greenwald limit) against deuterium gas fuelling in the various Mark IIA configurations. (b) Confinement enhancement relative to the ITERH93-P scaling law (H_{93}) as a function of deuterium gas fuelling for the discharges in (a).

For all configurations, the plasmas with Vertical Target (VT) strike zone positions are most tolerant to high fuelling rates. They are able to maintain their

confinement at higher values of fuelling, and reach their maximum density at higher fuelling rates (Fig.2). Thus they sustain a higher radiated power fraction with a less strongly deteriorated confinement. The radiated power fractions in a fuelling scan on VT plasmas at 2.5MA/2.5T with fixed beam power are shown in Fig.3(a). The radiated power reaches ~ 45% of the input power and the increase in radiation with fuelling comes entirely from the divertor region. In a reactor plasma this would be beneficial for target loading and erosion. The plasma purity also increases steadily in this scan (Fig.3(b)) partly offsetting the decline in H_{93}.

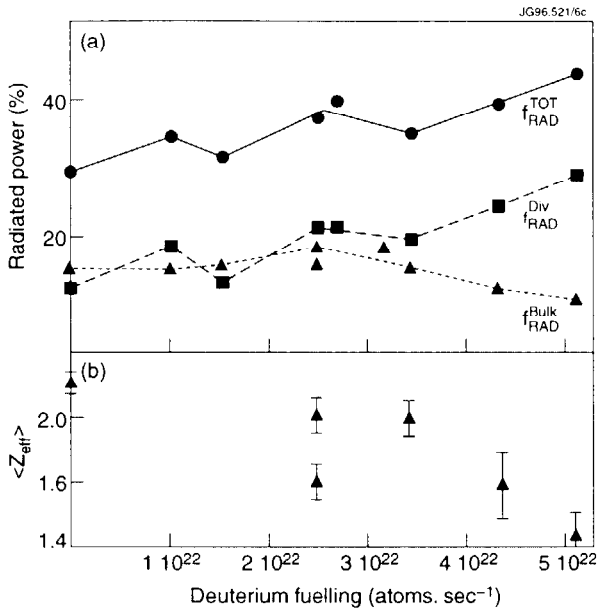

Fig.3 (a) Radiated power as a function of deuterium gas fuelling for the Vertical Target, higher triangularity discharges from the dataset in Fig.2. (Ip=2.5MA; B_T=2.5T; P_{nbi}=12MW). (b) Z_{eff} as a function of deuterium fuelling for the dataset of Fig.3(a).

The density limit in the Mark IIA configuration lies close to the Greenwald limit (Fig.4(a)). In contrast, with Mark I it was possible to exceed the Greenwald limit at low current (Fig.4(b)). There appears to be a trend towards a lower density limit as the divertor geometry becomes more closed. In the pre-1992 JET configuration with its open divertor, the Greenwald limit could be exceeded over a much larger range of I_p.

3. CONFINEMENT IN STEADY-STATE ELMY H-MODES AT HIGH CURRENT AND LOW q

ELMy H-modes lasting up to 10 energy confinement times have been obtained in diverted plasmas at plasma currents ≥ 4.5MA. An example of such a discharge is shown in Fig.5. Operation above 4.5MA in JET requires low q_{95} (≤ 2.5) as the toroidal field is presently limited to 3.4T. Thus optimisation of these plasmas is addressing a regime of particular interest to ITER.

It is found that energy confinement enhancement (H_{93}) does not degrade at low q in JET relative to the ITERH93-P law, but H_{93} in discharges with combined high current and low q (q_{95} ~ 2.4-2.5) is about 10% down on the mean values achieved at lower Ip. The energy confinement of ELMy H-modes with steady ELMy conditions lasting > $3\cdot\tau_E$ is shown in Fig.6 where H_{93} is plotted against q_{95}. The discharges above 4.5MA have a restricted triangularity range ($0.2 < \delta < 0.23$).

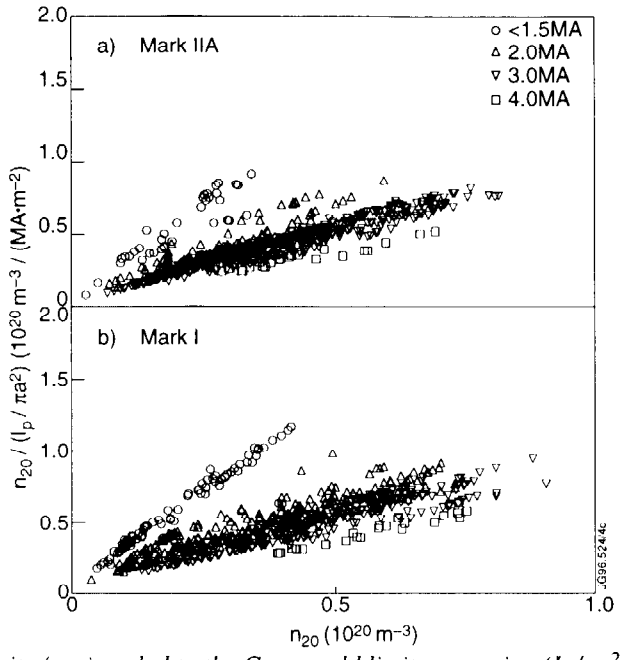

Fig.4 Plasma density (n_{20}) scaled to the Greenwald limit expression ($Ip/\pi a^2$) as a function of density and current for (a) Mark IIA plasmas; (b) Mark I plasmas.

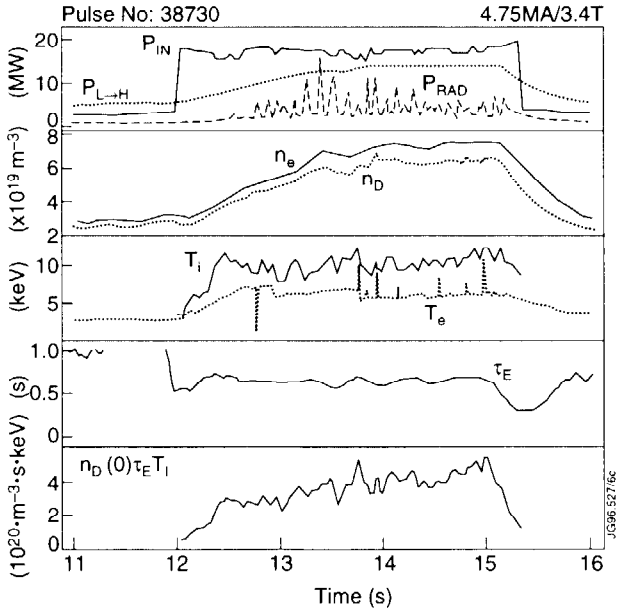

Fig.5 Time evolution of a steady-state type I ELMy H-mode at high current and low q (q_{95}~2.5).

Although good confinement can be achieved at low q, a significant number (~ 50%) of the ELMy H-modes produced at low q show a deterioration in confinement from one of two mechanisms.

i) Discharges with q_{95} ~ 2.4 are prone to the appearance of large n=2 MHD activity which, whilst the ELMy H-mode steady-state is maintained, leads to a loss of confinement by 10-15%. Examples of the steady-state confinement deterioration obtained are marked in Fig.6. It can be seen that

this is a low q rather than a high current phenomenon. These modes were present only rarely in Mark I. The nature of their appearance in Mark IIA is not yet understood, but the causal link with lack of confinement is clear.

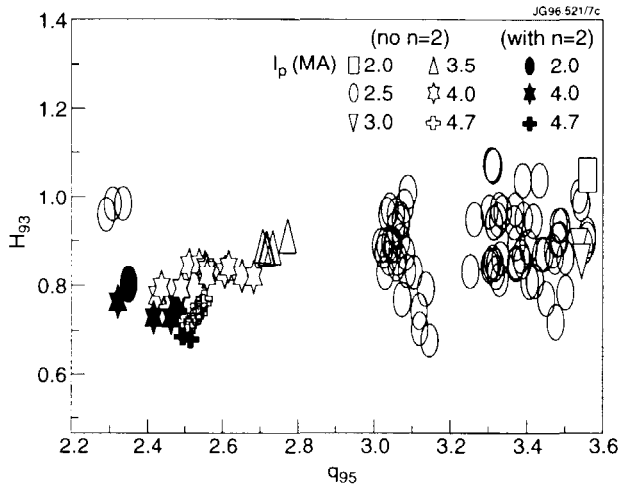

Fig.6 H_{93} as a function of q_{95} for steady-state ($\tau_H > 3 \cdot \tau_E$) ELMy H-modes. The solid symbols indicate discharges accompanied by strong n=2 MHD activity.

ii) Many discharges at $q_{95} < 2.6$ and $I_p > 4.0$MA suffer H-L transitions which occur randomly, frequently after many energy confinement times. A few of these discharges have input powers which are close to the L-H power threshold when bulk radiated power is subtracted. For the rest, the reverse transition occurs spontaneously and is accompanied by impurity influx and often by a slowly rotating or locked n=1 mode. These are generally thought to be effects of the loss of confinement rather than the causes. It is possible, at this early stage in the high current development, that the vessel has not been conditioned sufficiently for reproducible behaviour at high current and power.

Up to 25MW of combined heating power (17MW NBI and 8MW ICRF) has been coupled into JET plasmas at 4.7MA and 3.4T. The fusion triple product $n_D(o) \cdot \tau_E \cdot T_i(o)$ has reached ~ $4 \cdot 10^{20} m^{-3} \cdot s \cdot keV$ for three energy confinement times. Such plasmas would give a fusion amplification factor in D-T plasmas ($Q_{D\text{-}T}$) of around 0.25.

4. CONFINEMENT SCALING WITH DIMENSIONLESS PARAMETERS IN RADIATIVE DIVERTOR DISCHARGES

The scaling of energy confinement in discharges with a high fraction (> 50%) of radiated power, seeded by N_2 gas, has been studied in a series of plasmas which are dimensionally similar, except for the variation in normalised ion Larmor radius (ρ^*) and collisionality (ν^*). The aim of these experiments was to ascertain whether these ITER-relevant discharges are consistent with a gyro-Bohm scaling [6] such as ITERH93-P.

The time development of these H-mode discharges at 1MA/1T, 1.8MA/1.8T and 2.6MA/2.6T is shown in Fig.7. The discharges had the same q_{95} (=3.1), triangularity (δ ~ 0.3), minor radius, elongation and were all seeded by a mixture of N_2 and D_2 gas such that they reached a radiated power fraction ~ 60%. It can also be seen that they attained the same Z_{eff} of about 3.5. The input powers were adjusted such that the same thermal β_T was obtained (~ 1.3%). This involved scaling the input powers approximately as B^2. Due to the difficulty in adjusting the plasma density, ν^* was not kept constant from shot to shot, but varied by a

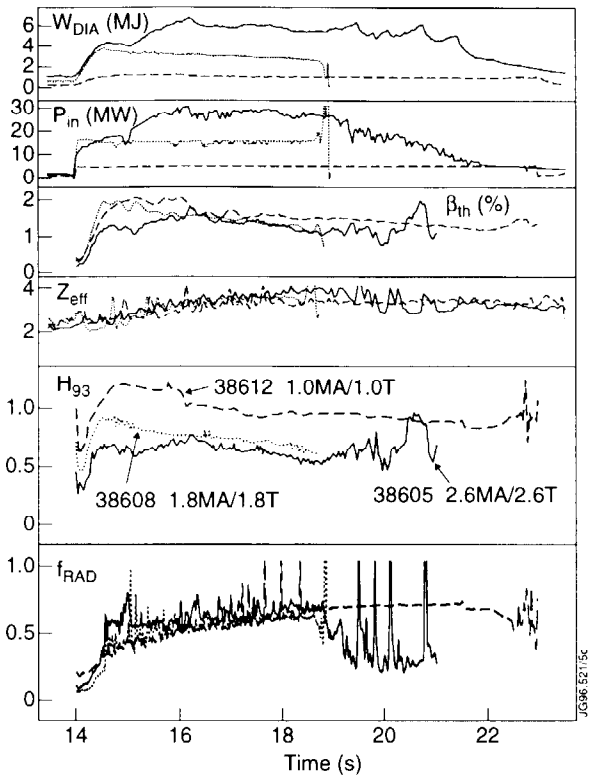

Fig.7 Comparative time evolution of stored energy; input power, thermal β; Z_{eff}; H_{93} and radiated power fraction for three discharges in the (ρ^*,ν^*) scan of radiative divertor plasmas.

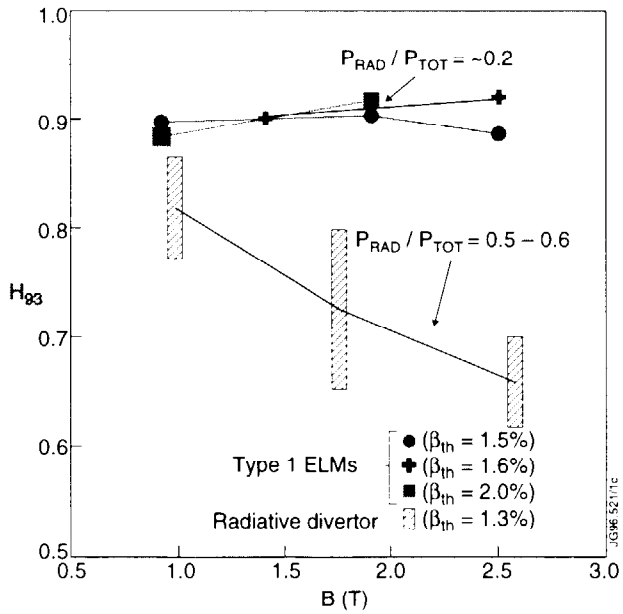

Fig.8 H_{93} as a function of toroidal field for the JET radiative divertor plasmas at similar (β, q, δ, κ, a, Z_{eff}, f_{RAD}). Also plotted are the type I ELMy H-modes from the ρ^* scan in JET (see [6]).

factor ~ 1.7. Since the collisionality scaling of ITERH93-P (gyro-Bohm like) and Bohm like scalings such as ITER89P are similar (~ $\nu^{*-0.3}$) the dataset should be capable of distinguishing the ρ^* scaling. The variation in ρ^* across the dataset is close to a factor 2.

It can be seen from the plot of H_{93} as a function of toroidal field in Fig.8 that confinement progressively decays relative to ITERH93-P as B increases. This is in contrast to the type I ELMy H-mode discharges in JET, which satisfy gyro-Bohm ρ^* scaling [6].

This data suggests that the radiative discharges are not consistent with a gyro-Bohm scaling law. Note also the tendency (Fig.8) for the confinement to approach the type I ELMy discharges at low toroidal field (higher ρ^*).

5. CONCLUSIONS

The scaling of density with power and current in ELMy H-modes in the Mark IIA divertor without added gas fuelling is similar to that seen in Mark I.

With gas fuelling, confinement progressively degrades from equality with the ITERH93-P scaling law. This degradation may be due to interaction caused by increased midplane pressure and recycling which occurs at high gas fuelling due to bypass leaks from the divertor region.

The vertical target plasmas are most tolerant of gas fuelling, maintaining their confinement to higher fuelling rates and producing radiative power fractions of 40-50% with good plasma purity.

There is a maximum density for gas fuelling in any particular plasma configuration. As fuelling rates are increased further the plasma density declines. It has not yet been possible to exceed the Greenwald limit in Mark IIA although operation close to this limit has been possible. The density limit appears to be an inability to maintain fuelling efficiency because of increased ELM activity. JET data supports the conclusion that the density limit becomes lower as divertor closure improves.

Confinement does not degrade relative to the ITERH93-P scaling law at low q in steady-state ELMy discharges. There is a slight degradation at high current but this may be due to insufficient conditioning at high current and power. Low q discharges are more susceptible to n=2 MHD activity in Mark IIA than in Mark I. There is also a significant increase in the number of low q, high current discharges with unexplained reverse H→L transitions.

The confinement scaling in JET radiative divertor ELMy H-modes at constant shape, q and β is not consistent with a gyro-Bohm scaling such as ITERH93-P. Further work is needed on truly dimensionless discharges in this regime to determine the precise dependence on ρ^*.

6. REFERENCES

[1] THE JET TEAM (presented by G. Vlases), IAEA-CN-64/A4-1, this Conference.

[2] THE JET TEAM (presented by G. F. Matthews), Plasma Phys. and Control. Fus. **37**, 227 (1995).

[3] STORK, D. et al., in Controlled Fusion and Plasma Phys. (Proc. 22nd Eur. Conf. Bournemouth, 1995) Vol. 19C Part II (1995) 125.

[4] THE JET TEAM (presented by L.D.Horton), paper presented at 23rd Eur. Conf. Kiev, 1996 (to be published in Plasma Phys. Control. Fusion).

[5] SAIBENE, G. et al., to be published in J. Nucl. Mater. (Proc. 12th Int. Conf. on Plasma Surface Interactions, St Raphael, 1996).

[6] The JET TEAM (presented by J. G. Cordey), IAEA-CN-64/AP1-2, this Conference.

HIGH FUSION PERFORMANCE ELM-FREE H-MODES AND THE APPROACH TO STEADY OPERATION

The JET Team[1]
(Presented by PJ Lomas)

JET Joint Undertaking,
Abingdon, Oxfordshire,
United Kingdom.

Abstract

The highest fusion yield in JET has been obtained in the hot ion H-mode regime. This paper reports progress in fusion performance in this regime. Since the last IAEA conference the fusion performance on the MKI pumped divertor has been doubled, with D-D neutron rates up to 4.65 10^{16}n/s demonstrated, equivalent to $Q_{DT} \sim 1$, similar to the PTE-1 series. More recently a more closed divertor MKII has been installed, and the new results will be described.

1. BASIC FEATURES OF THE REGIME

Figure 1 shows a typical hot ion H-mode plasma obtained with the new MKII divertor. After formation of the X-point the density is allowed to pump out to ~$1x10^{19}m^{-3}$ before the application of high power neutral beam (NB) heating. After a period of threshold ELMs the plasma becomes ELM-free, during which time both stored energy and D-D neutron rate increase steadily. The ion temperature, on the other hand, reaches a maximum and then declines somewhat as the density continues to increase. The loss power, P_{NB}-dW/dt-P_{SH} (where P_{SH} corresponds to the calculated shine through power), increases with time as does the stored energy, indicating approximately constant confinement time. The high performance phase is limited in this case by beam switch off followed 50ms later by a giant ELM and sawtooth (coincident to within 100μs). These and other limitations to performance are discussed in [1].

The duration of the ELM free phase is similar on both MKI and MKII for similar core plasma shapes, edge shear, $S_{95} \gtrsim 3.5$, triangularity, $\delta \gtrsim 0.3$. Higher triangularity configurations have been tested up to $\delta \sim 0.6$, $S_{95} \sim 4.0$ at 2.5MA but have not demonstrated any significant improvement in confinement quality. Configurations with low edge shear $S_{95} \lesssim 3$ and low triangularity $\delta \lesssim 0.2$ show repetitive giant ELM's with frequencies $\gtrsim 5Hz$.

Given the similarities in plasma behaviour in MKI and MKII it is not surprising that the fusion performance of the NB only data is also similar at the same beam power and shows the same strong scaling with NB power as illustrated in Fig.2. Thus far, for technical reasons, the NB power on MKII has been limited to <17MW, but this deficiency is being corrected, and this is expected to restore the MKI performance later this year. Note also that steady neutron yields can be maintained for about 1s by step-down of the beam power to the level of the loss power in the preceding transient phase.

---

[1] See Appendix to IAEA-CN-64/O1-4, The JET Team (presented by J Jacquinot).

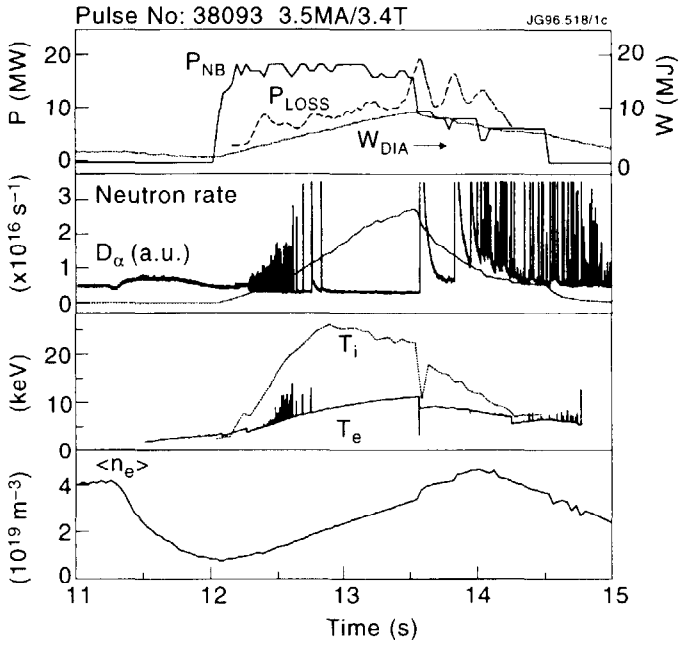

Fig.1 Typical time traces for an hot ion plasma showing neutral beam power P_{NB}, loss power P_{Loss} (see text), diamagnetic stored energy W_{DIA}, D-D neutron rate, D_α, ion and electron temperatures T_i and T_e and volume averaged density <n_e>.

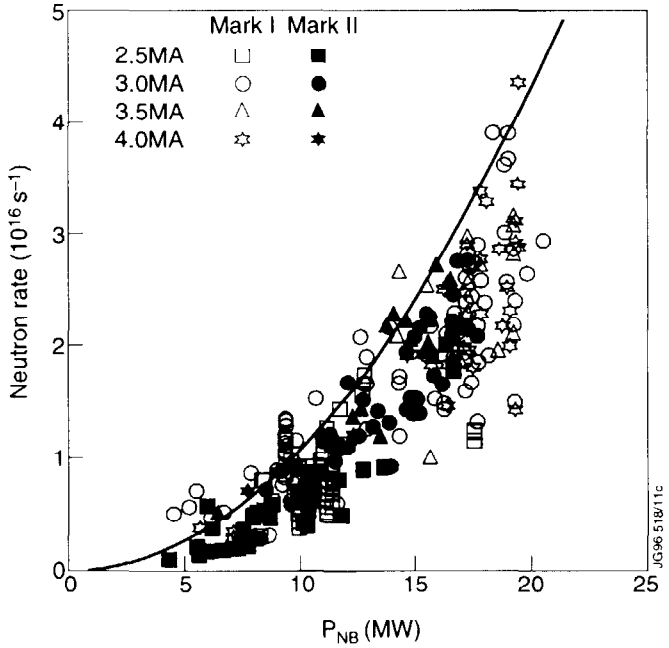

Fig.2 Neutron rate plotted against total neutral beam power. Open symbols refer to MKI and closed symbols refer to MKII. The shape of the symbols indicate plasma current: squares 2.5MA, circles 3MA, triangles 3.5MA and stars 4MA.

2. THE TRANSPORT BARRIER

A model has been developed [2] which accounts for many of the features observed in JET ELM-free H-modes. The model assumes:- (1) transport inside the barrier region is given by ion neo-classical together with anomalous terms including both Bohm (global) and gyro-Bohm terms, (2) transport coefficients within the transport barrier $D \sim \chi_i \sim \chi_e \sim \chi_i^{neocl}$ are given by the ion neo-classical diffusivity and (3) the width of the transport barrier is given by the ion poloidal banana width $\Delta \sim \sqrt{\varepsilon}\rho_{\theta i}$. Note that the Bohm terms dominate the transport in the outer regions of the plasma up to the transport barrier and the gyro-Bohm terms dominate the central confinement.

With these assumptions it is possible to construct a complete set of transport equations for n_e, T_e, T_i and J which can be solved self consistently. A single free parameter remains which can be the edge density (or alternatively the net recycling coefficient) which is adjusted to match the observed density evolution. When applied to hot ion plasmas the time evolution of plasma parameters and profiles are well reproduced. In particular, the initial linear rise in stored energy is well described, and is followed by a progressive saturation which the model suggests is due to the density rise. The model describes accurately the evolution of power step-down pulses and the effect of strong gas puffing, and can account qualitatively for the temporary degradation of confinement following a sawtooth crash. The code predicts the time when ballooning modes become unstable which is consistent with the experimentally observed appearance of giant ELM's as shown in Fig.3. Indeed, this confirms, in a very satisfying manner, that the transport is close to ion neo-classical in the barrier region because an increase in transport would lead to ballooning modes always being stable.

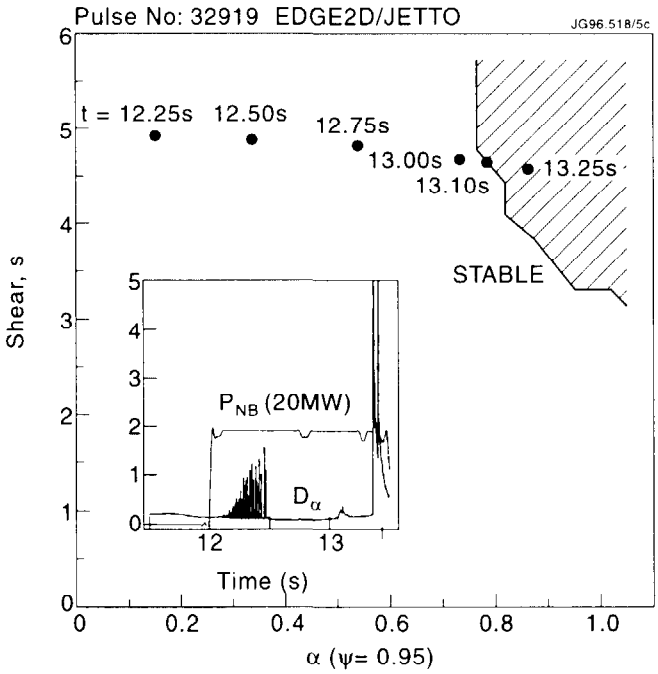

Fig.3 Trajectory of the model simulation of pulse 32919 in the S-α (shear versus normalised pressure gradient) diagram. The ballooning unstable region is shown shaded. Ballooning instability is predicted at 13.1 s which should be compared with the ELM time of 13.4 s shown in the inset.

Measurements of both ion and electron temperature profiles across the transport barrier are shown in Fig.4(a). The transport barrier is most clearly defined in the electron temperature data and this width is plotted against the best fit in Fig.4(b). Note that this result does not conform to the expected scaling $T_i^{1/2}/I_p$. Further analysis is in progress which may resolve these discrepancies, but it may be necessary to include more physics elements such as the penetration depth of cold neutrals. The first attempt to self consistently compute the scrape-off layer (SOL) and core transport together with neutral penetration is described in [3].

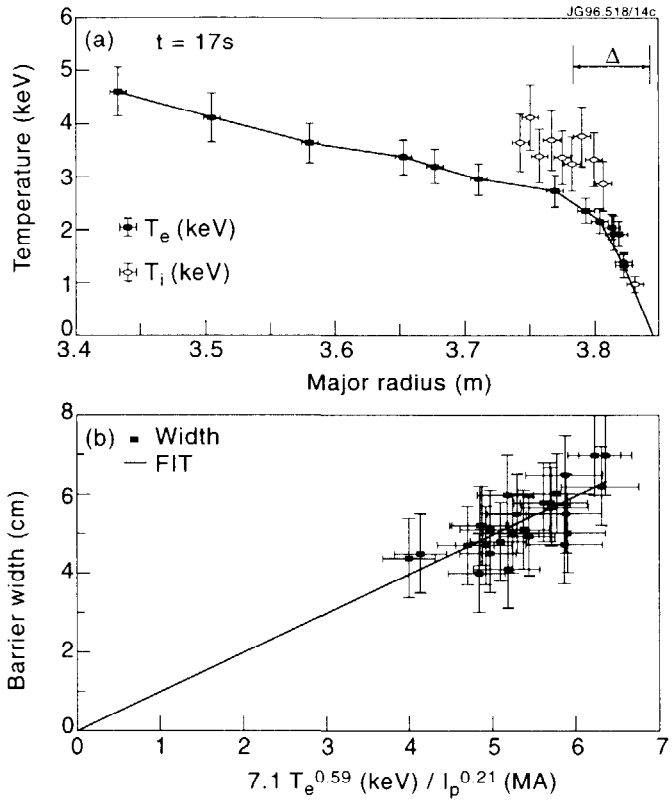

Fig.4 (a) Ion and electron temperature profiles for pulse 37444 (2.6MA/2.54T) from which the transport barrier width Δ is determined. (b) barrier width against fitted dependence on temperature and plasma current. Note the weak dependence on I_p.

3. THE ROLE OF RECYCLING

It was already described at the last IAEA conference [4] how the main chamber recycling plays an important role influencing both ELM-free period and performance. Simulations with the model described above confirm this sensitivity. The distribution of the D_α light clearly shows the brightest signals from the divertor strike zones but reveals some contribution from the inboard (small major radius) plasma edge.

Measurements of Zeeman split D_α on a horizontal chord indicates approximately 4 times the light from the small major radius side of the plasma compared to the large major radius side.

In order to quantify the relative contribution of recycling in the main chamber compared to the divertor a selective hydrogen loading experiment was performed. The measured H/H+D fraction determined from vertical chord H_α and D_α is shown in Fig.5 as a function of pulse number for 4 sequences of pulses repeated on two successive days.

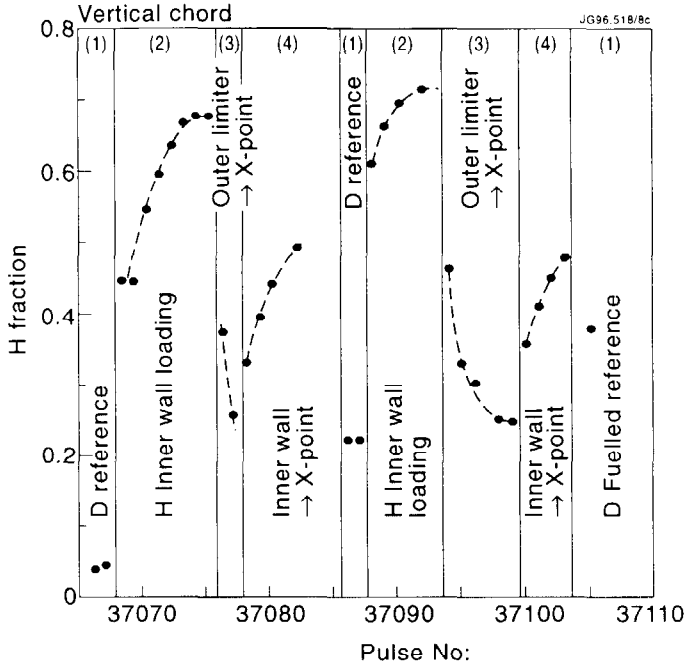

Fig.5 Ratio of H/H+D from H_α, D_α light measured on a vertical chord for a series of pulses from the selective hydrogen loading experiment (see text). Where the plasma pulse includes both limiter and X-point phases the measurement is taken during the deuterium beam fuelled H-mode in the X-point phase. The figure shows two cycles of experiments 37066-37084 and 37086 - 37105 repeated on successive days.

The sequence of pulses are as follows (as labelled on Fig.5). (1) reference pulse with deuterium gas fuelled inner limiter phase followed by deuterium beam fuelled H-mode, (2) inner wall limited pulses with hydrogen gas fuelling (3) pulses with deuterium gas fuelled outboard limiter phase followed by deuterium beam fuelled H-mode (4) pulses with hydrogen gas fuelled inner wall limiter phase followed by deuterium fuelled H-mode. For clarity the data points in Fig.5 represent the X-point phase when there is more than one phase. Generally the hydrogen concentration is low during the outboard limiter phases of sequences (1) and (3). The H/H+D ratio during the inner wall hydrogen loading pulses (2) behaves in a similar manner to previous isotope exchange experiments [5]. Note that sequence (3) has no direct contact with the inner wall and its inventory of hydrogen, and yet the X-point phase starts with an high concentration of hydrogen which decreases pulse by pulse. In sequence (4), where the hydrogen concentration is topped up during the inner wall phase, the concentration during the X-point phase increases pulse by pulse. These results demonstrate that there is significant exchange, during the H-mode phase only, of hydrogen from the inner wall to the divertor target and of deuterium from the divertor target to the inner wall. Thus a significant fraction (0.25 - 0.5) of the recycled particles originate

from the inner wall, demonstrating the importance of the main chamber recycling during diverted H-modes.

The more closed MKII divertor was predicted to increase the pressure of neutrals in the diverted region and hence increase pumping. The data in Fig.6 clearly shows the increase in pumping during ELM-free H-modes in MKII compared with MKI. Indeed in MKII the density rise during the ELM-free H-modes is reduced by ~ 30% such that it is necessary to add gas to optimise the fusion yield (minimise NB shine through losses and Z_{eff}). At low gas puff there is a clear net source of particles from either walls or target whereas at sufficiently high gas flow these surfaces provide a net pump. Alternatively these results can be thought of as a decrease in gas fuelling efficiency (from ~ 50% to $\leq$ 10%). This strong divertor pumping has reduced the need for extensive conditioning for access to the hot ion regime and increased the reproducibility of the performance achieved but has not, as yet, significantly improved the performance or confinement quality.

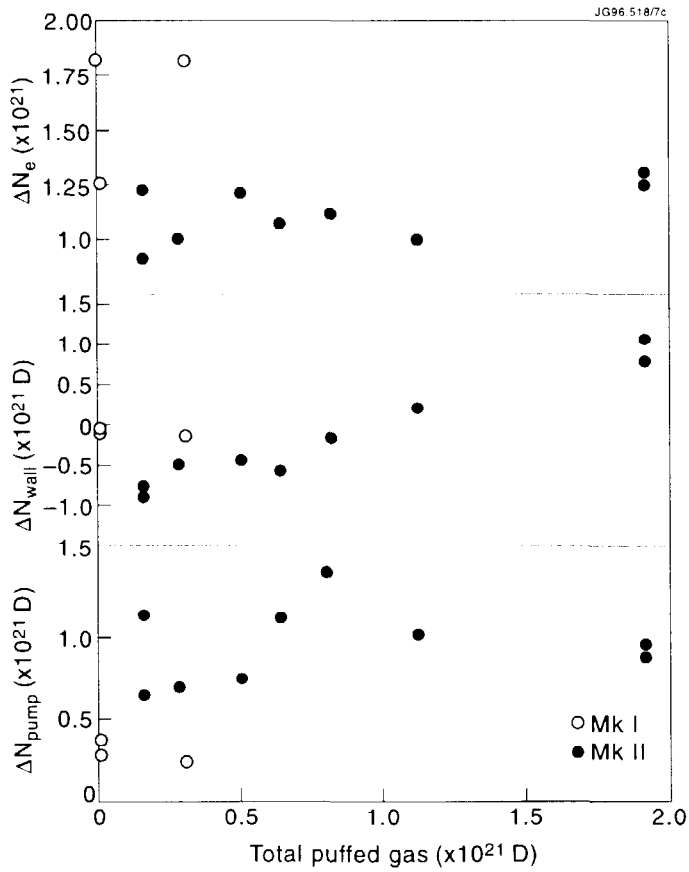

Fig.6 Particle balance over the first second of neutral beam heating for a series of ELM free H-modes. The change in plasma particle inventory, wall inventory and pump inventory are shown as a function of total gas puffed in the same interval. Open symbols refer to MKI and closed symbols refer to MKII. The neutral beams inject 17MW and 1.4 10^{21} particles per second.

4. COMBINED HEATING

Ion cyclotron resonance heating (ICRH) has been coupled in conjunction with NB heating to produce ELM-free H-modes with combined heating (NBRF). The coupling resistance falls during the ELM-free H-mode from about 2Ω to 1.5Ω. Nevertheless, it has been possible to couple up to 9.5MW. Together with NB a total power up to 25MW has been applied for plasma currents up to 3.8MA generating stored energies up to 14MJ. The diamagnetic energy confinement time $\tau = W_{dia}/(P_{NB} + P_{RF} - dW/dt)$ is about 1 s in these cases, similar to the NB only cases, suggesting no strong effect according to different proportions of electron and ion heating.

Figure 7 compares high D-D yield pulses at similar NB power with and without 6.5MW of ICRH resonant on axis with hydrogen and second harmonic deuterium. The increase in stored energy, D-D neutron yield, ion and electron temperatures are clear, and the shorter ELM-free phase is as expected. The high energy neutral particle analyser clearly shows the generation of a deuteron tail with energies up to 1MeV, as expected from PION code calculations. Neutron accounting using kinetic data suggest increased neutron production from both thermonuclear and non-thermal reactions. With added hydrogen or mixed

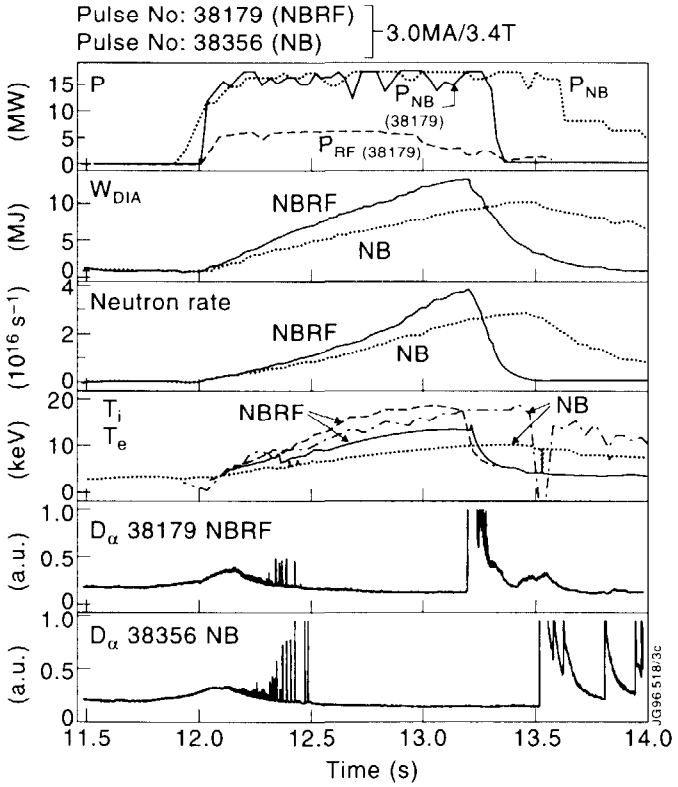

Fig.7 Typical time traces comparing NB only (38356) and combined heating NBRF (38179). The traces shown are input powers, P_{NB}, and P_{RF}, diagmagnetic stored energy W_{DIA}, neutron rates, ion and electron temperatures and D_α

frequency (multiple resonance position) ICRH the observed tail can be smaller by an order of magnitude and yet still the D-D neutron rate is increased over and above the NB only cases. These results suggest a useful increase in fusion yield when ICRH is applied to DT plasmas, but it is too early to make quantitative predictions.

5. DT EXPECTATIONS

The best NB only plasma in MKI has demonstrated $n_D(0)\tau_E T_i(0) \sim 8.8\times10^{20}$ and TRANSP analysis indicates $Q_{DT}^{equiv} \sim 1$ (with the definition in [6]). High performance can be sustained for about 1 s by stepping down the NB power to about the loss power and in such cases $Q_{DT}^{equiv} > 0.8$ for 1s. Similar results are expected with MkII when the full beam power is restored later in 1996.

These extrapolations assume that 50:50 D:T mix can be achieved. By operation of the tritium beams at full power and the deuterium beams at reduced power 20 MW can be delivered with comparable deuterium and tritium fluxes. Provided that the core is dominated by beam fuelling a 60:40 mix should be readily achievable. Contributions to the core D-T mix from recycling could be offset by tritium beam prefuelling or gas puffing. Operation of the deuterium beams at full power would deliver ≃ 23MW and would be expected to increase the D-T neutron yield by up to 30% provided that the shortfall in tritium fuelling can be made up (by gas puffing or prefuelling).

6. CONCLUSIONS

The behaviour of the hot ion ELM-free H-mode regime is reassuringly similar in the MKI and MKII divertor. Improved pumping has reduced the characteristic density rise and increased operational flexibility, but has not as yet led to any significant improvement in performance. Similar high fusion performance, as already demonstrated on MKI, is expected on MKII when the neutral beam power is restored. Improved performance has been demonstrated with the addition of ICRH power to the hot ion ELM-free regime. The transport model continues to describe the main features of this regime and recently detailed edge temperature measurements have been made which should enable a refinement of the physics of the transport barrier.

Last, but not least, the rapid progress so far achieved with the MKII divertor shows great promise for the forthcoming DT experiments.

REFERENCES

[1] THE JET TEAM (presented by P. R. Thomas), IAEA-CN-64/A3-2, this Conference.

[2] BAK, P., et al., Nucl. Fusion **36** (1996) 321.

[3] THE JET TEAM (presented by A. Taroni), IAEA-CN-64/D3-3, this Conference.

[4] THE JET TEAM (presented by P. J. Lomas) in Plasma Physics and Controlled Nuclear Fusion Research 1994 (Proc. 15th Int. Conf. Seville, 1994) Vol. 1, IAEA, Vienna (1996) 211.

[5] HORTON, L.D., et al., J. Nucl. Mater. **196-198** (1992) 139.

[6] BALET, B., et al., Nucl. Fusion **33** (1993) 1345.